Journal of Inorganic and Organometallic Polymers and Materials (2021) 32:1223–1233
https://doi.org/10.1007/s10904-021-02171-2

Facile Synthesis and Antibacterial Activity of Bioplastic Membrane Containing In Doped ZnO/Cellulose Acetate Nanocomposite

M. S. Aida[1] · N. H. Alonizan[2] · M. A. Hussein[3,4] · M. Hjiri[1] · O. Abdelaziz[5] · R. Attaf[6] · B. Zarrad[1]

Received: 18 October 2021 / Accepted: 21 November 2021 / Published online: 28 November 2021

Abstract

The present work addresses a facile synthesis of Indium doped zinc oxide (IZO) cellulose acetate nanocomposite membrane. The membrane was prepared by casting method. Various weights of In:ZnO nanoparticles were added to solution formed by dissolution of cellulose acetate granules in acetone. The harvested membrane, after acetone evaporation, was characterized by various techniques including X ray diffraction, scanning electron microscopy, energy dispersive X ray and elemental mapping, Fourier transform infrared spectroscopy. The results show that the In:ZnO nanoparticles are well embedded in the cellulose acetate host matrix. The elemental mapping reveals that the nanoparticles are uniformly distributed. The optical characterization reveals the reduction of the transmittance in the UV (A and B range) of the CA/IZO composite with increasing the weight of the added IZO powder. This reduction was attributed to ZnO UV absorption. No noticeable peak assigned to ZnO bond are observed. However, IR peaks are shifted towards the higher wavenumber due to the change of the bonds environment with including IZO in the CA matrix. The antibacterial action of the synthetized nanocomposite membranes was tested against *Escherichia coli* (*E. coli*). *Staphylococcus aureus* (*S. aureus*). The assay results have shown that the membrane has no activity against (*E. coli*). In contrary, the synthetized membrane exhibits an interesting antibacterial activity against *S. aureus*. The inhibition region varies from 6 to 15 mm with increasing the weight ratio of filler. A zone of inhibition (ZOI) of 18 mm was observed for the membrane prepared with 30% wt. of In:ZnO. We noticed that the ZOI radius increases with the added weight of IZO. Due the settling down of the nanoparticles only one face of the membrane exhibits an antibacterial activity.

Keywords Facile synthesis · Bioplastic membrane · Antibacterial activity · In doped ZnO nanoparticles · Cellulose acetate

1 Introduction

Hybrid polymeric nanocomposite films have gained increasing attention during the last decade, due to their interesting and promising physical, chemical, and optical properties [1–4]. Merging metal or metallic oxide nanoparticles with polymers leads to the improvement of the physicochemical properties and behavior of the polymer [5]. Hence, the produced composites represent a new class of materials suitable for applications in several fields [6–14]. A large variety of polymers have been used for the production of various composite materials with interesting mechanical properties, thermal stability, biocompatibility, and high chemical resistance. These unique characteristics of nanostructured composites were a reasonable stimulus for the researcher and industrial activity in the polymer based nanocomposite. The most commonly used composite are produced by the combination of polymer matrices including poly(methyl

✉ M. S. Aida
aida_salah2@yahoo.fr

[1] Department of Physics, Faculty of Science King, Abdulaziz University, Jeddah, Kingdom of Saudi Arabia

[2] Department of Physics, College of Science, Imam Abdulrahman Bin Faisal University, P.O. Box 1982, Dammam 31441, Saudi Arabia

[3] Chemistry Department, Faculty of Science, King Abdulaziz University, P.O. Box 80203, Jidda 21589, Saudi Arabia

[4] Chemistry Department, Faculty of Science, Assiut University, Assiut 71516, Egypt

[5] Laboratoire de Biochimie Appliquée, Faculté des Sciences de la Nature et de la Vie, Université Frères Mentouri Constantine, Constantine, Algeria

[6] Department de Physique, University Mentouri Constantine 1, 25000 Constantine, Algeria

methacrylate), polycarbonate, polystyrene and thermosets (e.g., epoxy, silicone) with various inorganic fillers in particular oxides namely: SiO_2, TiO_2, CeO_2, ZnO, ferric oxide, semiconductors: CdS, PbS, CdTe, CdSe, minerals: clays, $CaCO_3$ and metal: Au, Ag, Cu, Ge, Fe) [10]. Among these polymers, the cellulose acetate (CA) based materials have attracted an increasing interest. Cellulose with a chemical formula $(C_6H_{10}O_5)_n$ is a commercially available, naturally obtained polymer [15–19]. Cellulose acetate biopolymer is characterized by its high mechanical strength, good biocompatibility, biodegradability, hydrophilicity properties [20, 21], thus making it highly desirable in numerous biomedical, antibacterial applications and wound healing [22–28]. Recently, wound-healing properties of numerous metal nanoparticles have been demonstrated [29]. Substantial research attention has been paid to metal and metal oxide nanoparticles (NPs) due to their exceptional physical properties, this have enabled their broad use in diverse applications [30–33]. These nanoparticles particles embedding into a polymer matrix yields to original composites with new properties owing the advantages of both components. Beisl et al. [34] have prepared cellulose acetate with silver nanoparticles to improve their antibacterial properties. Amin et al. [35] have added TiO_2 to the mechanical properties of bioplastic. Al Saeed et al. [36] prepared scaffold base on CA loaded with copper oxide nanoparticles. They noticed and improvement in the plastic hydrophilicity beside its ability to kill infectious microbes abundant in wounds. Jatoia et al. [37] have synthetized a composite formed by carbon nanotubes and silver nanoparticles incorporated into polymer matrix with the goal to minimize the direct contact of silver nanoparticles with human cells to reduce silver leaching. Matosa et al. [38] have produced composite membranes by combining magnetic nanoparticles with cellulose acetate membranes for magnetic hyperthermia application. Ahmed et al. [39] have introduced ZnO, Ag and CuO nanoparticles into of cellulose acetate and ε-olycaprolactone matrix blend. They investigated the synthetized composite viability and antibacterial activity against *Staphylococcus aureus* (*S. aureus*) and *E. coli*. Alay et al. [40] have prepared a nanocomposite via combination of nanostructured zinc oxide (ZnO) and graphene oxide with cellulose acetate (CA). They reported that this combination yields to some good bio-composite materials for wound healing application. Fahmi et al. [41] have synthetized nanocomposite membrane composed of cellulose acetate and collagen matrix blend embedded with $MnFe_2O_4$ nanoparticles and apply it in drug delivery. Kalaycıoğlua et al. [42] have prepared a wound dressing composite materials composed of cerium oxide nanoparticles introduced into chitosan and cellulose acetate polymer matrix. Baday et al. [43] have decorated cellulose acetate nanocrystals during the synthesis with Ag and ZnO nanoparticles. The obtained nanocomposites, have been experienced as some effective adsorbents for lead ion Pb(II). Haider et al. [44] have synthetized cellulose acetate nanofibers decorated with CuO nanoparticles and apply them as a potential wound dressing material, they exhibited excellent antibacterial efficacy against both *E. coli* and *S. aureus* bacteria's. Zinc oxide nanoparticles have been studied extensively in the past years. Their unique properties enable their multidisciplinary applications in several industrial fields [45–49]. Therefore, developments of nanoparticles with antimicrobial properties are of considerable interest. In the last few years, multifunctional metals and metal oxides have attracted interest for their antimicrobial activities. Metal oxide nanoparticles find many applications in physical, chemical and biological fields. Metal oxides nanoparticles, such as TiO_2, ZnO, CuO, SiO_2, SnO_2 and MgO have proven an interesting antibacterial properties. ZnO has attracted a special interest due to its application in health care products, UV radiation blocking. The antibacterial activity of ZnO NPs was reported earlier [50, 51]. It has been demonstrated that ZnO nanostructures can be successfully used against both Gram-positive and Gram-Negative bacteria [52, 53]. Due to their interesting properties, ZnO nanoparticles can be introduced into polymers matrix in order to tune polymers properties that may covers a wide area of applications. To the best of our knowledge, the incorporation of Indium doped ZnO in CA matrix is not studied.

The preset work deals with the synthesis of nanocomposites by incorporating IZO nanoparticles into CA matrix. The antibacterial activity of the synthetized nanocomposite is investigated. The structural, compositional properties of the synthetized composite is firstly investigated and the antibacterial activity against *E. coli* and *S. aureus* bacteria's is also addressed. During the IZO/CA composite preparation, the ratio of the nanoparticle mass, regarding the biopolymer, was varied in order to investigate the effect of nanoparticles concentration.

2 Experimental Details

2.1 Nanoparticles Preparation

In-doped ZnO nanoparticles were prepared via sol gel technique. The starting solution was prepared by dissolving zinc acetate dehydrate $Zn(CH_3COO)_2{\cdot}2H_2O$ (Sigma-Aldrich, > 99.5% purity) in methanol with a 0.1 M molarity. The weight of the added dopant source indium chloride $InCl_3$ (Sigma-Aldrich, > 99.5% purity) is calculated to achieve the desired In/Zn ratio of 3 at%. After stirring for 10 min at room temperature, the solution was placed in an autoclave heated at supercritical condition at 250 °C for 10 h. The resultant material was washed several times with mixture of ethanol and water for purification and then dried

at 60 °C for 1 h in an oven. The harvested nanopowder was then calcinated at 400 °C for 2 h in an open oven.

2.2 Nanocomposite Fabrication

Cellulose acetate was purchased from BDH, (Germany, 99%) and was used as received without any additional treatment. 2 g of CA granules were dissolved in 20 ml pure acetone. IZO nanopowder was added to the dissolved CA solution. A set of IZO/CA bioplastic films were prepared by varying the weight percentage of the added IZO nanoparticles regarding the CA mass, the used weigh ratios were 5, 10, 15 and 25%. The solution was mixed in a beaker and ultrasonically treated to obtain a well-dispersed and homogeneous solution. A glass petri dish was then filled with the obtained solution for casting. The dish was covered with aluminum foil to avoid any environmental particles contamination. The solution was dried during 24 h at room temperature, the bioplastic film is formed after acetone evaporation.

2.3 Nanoparticles and Biopolymer Characterizations

The structure of the prepared In doped ZnO nanoparticles and IZO/CA composite were characterized by X-ray diffraction (XRD) using X'pert Pro diffractometer using the Cu-Kα radiation in the 2θ range from 20° to 80°. The nanoparticles and IZO/CA films morphology was analyzed by mean of scanning electron microscopy (SEM) observations using Zeiss Cross Beam 540 instrument, equipped by an energy dispersive X ray (EDX) spectrometer for elemental analysis and element mapping. The transmission optical properties, of the IZO/CA polymer films were acquired via the UV–Vis spectrophotometer (Bio Aquarius CE 7250, UK). The Fourier transform infrared (FTIR) absorption coefficients of the bioplastic films were measured using a Brucker spectrophotometer in the wavenumber range 400–4000 cm^{-1}.

2.4 Antibacterial Activity

The antibacterial activity assay of the obtained bioplastic films was evaluated by disk diffusion method regarding Gram positive (*Staphylococcus aureus* (ATCC 43300)), and Gram negative species (*Escherichia coli* ATCC 25922)).

The prepared IZO/CA films were cut into disk specimens (diameter of 6 mm). The cut discs were washed with distilled water and sterilized at 120 °C/20 min. Thereafter, 100 µl of bacterial inoculums with a concentration of 10^8 CFU/ml, have been served on plates containing Mueller Hinton agar. The testing discs are then placed on the surface of the media. Thereafter, the plates have been incubated for 24 h to 48 h at 37 °C. The diameters of inhibition zones were measured to assess the antibacterial activity.

3 Results and Discussion

Figure 1 represents XRD diffraction pattern recorded for In-doped ZnO synthetized nanopowder. As can be seen, the obtained nanopowder is polycrystalline, its XDR pattern is composed of different peaks assigned to the diffraction plan (100), (002), (102), (110), (103) and (112) of the ZnO Wurtzite hexagonal structure (according to JPCD card No. 36–1451). No other secondary peaks originating from In related phases such In_2O_3 or In metallic was observed. This indicating the pure quality of the synthetized nanopowder and also that In is incorporated and diluted in the ZnO lattice and do not form any secondary phases, confirming thereafter the In doping success of ZnO nanoparticles. The crystallite size is calculated using Hall–Williamson method. The estimated crystallite sizes were in the order of 34.2 nm.

The nanopowder morphology was studied using SEM observation. Figure 2a shows the SEM images of In-doped ZnO nanopowder. The nanopowder is composed of agglomeration of spherical nanoparticles. To confirm the In incorporation, we have reported in Fig. 2b the recorded EDX spectra in IZO nanopowder, as can be deduced the synthetized nanoparticles are composed of the element Zn, O and In necessary for IZO formation.

Figure 3 represents the XRD pattern of bioplastic IZO/CA films composite prepared with different IZO weigh ratios. The peaks related to ZnO phase appears with IZO filler adding. The ZnO peaks intensities increase with increasing the mass of the added ZnO nanoparticles. An interesting feature is the emergence of the same peaks assigned to the diffraction plan (100), (002), (102), (110), (103) and (112) of the ZnO Wurtzite hexagonal structure as observed in the IZO nanoparticles (Fig. 1). For the pure CA XRD diffraction pattern is composed with a broad peak confirming its amorphous structural nature.

The SEM images of the synthetized bioplastic composite are shown in Fig. 4a–d. At 5% of added filler mass ZnO nanoparticles image starts to be visible. At higher ratio 15 and 25% the SEM images reveals clearly the presence of the added ZnO nanoparticles. The aspect of the nanoparticles is comparable to that observed in the starting IZO nanopowder (Fig. 2a). This suggests that the added IZO nanoparticles are imbedded in the CA matrix.

To assess the uniform distribution of the IZO nanoparticles in the host matrix, we have proceeded with elements mapping (Fig. 5a–d) and EDX composition in three different region (Fig. 5e, f) in the IZO/CA film prepared with a mass ratio of 15% taken as example. Figure 5a–d show the different element forming the IZO nanoparticles. The elements In, Zn and O, as can be deduced from these figures, are well uniformly distributed in the whole film regions.

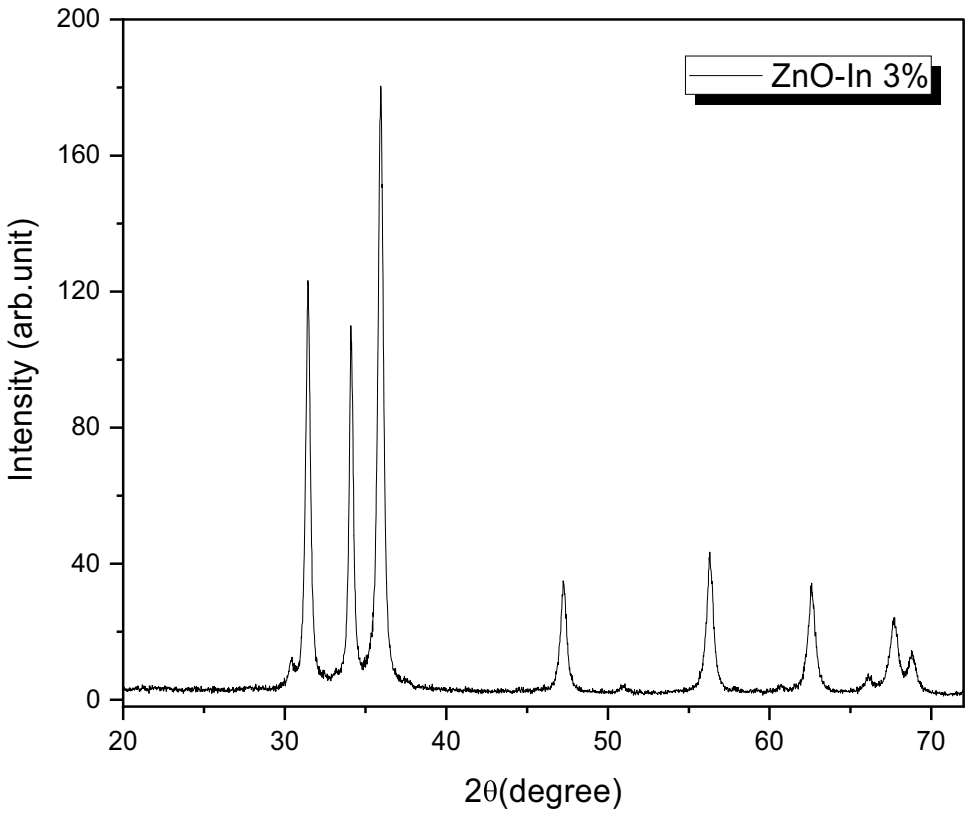

Fig. 1 XRD diffraction pattern of the synthetized In doped ZnO nanoparticles

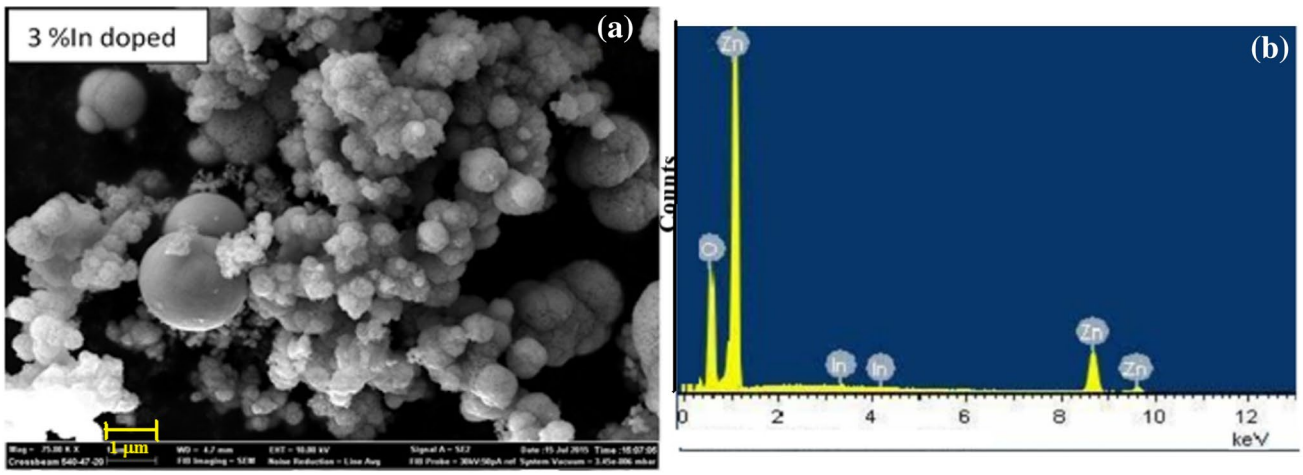

Fig. 2 SEM image (**a**) and EDX spectrum (**b**) of In doped ZnO nanoparticles

The films transmittance spectra in the UV–Vis range are reported in Fig. 6. The film transmittance variation in the visible range 400 to 800 nm can be explained in term of the film thickness. The absorption threshold is red shifted with increasing the IZO weigh concentration. Indicating the band gap reduction from 3.26 to 3 eV of the IZO/CA composite with increasing the weight ratio of ZnO introduced in the polymer matrix as shown in the insert Fig. 6. Culicia et al. [54] have investigated the effect of CeO_2 nanoparticles on the optical properties of the CA polymer and their UV filtration, they reported a reduction of the band gap from 3.36 to 3.28 eV with increasing the concentration of CeO_2 filler in CA matrix. The CA based nanocomposites can be used for photocatalysis for waste water treatment, this reduction in the composite band gap can be benefit for this technique. This may lead to energy consumption reduction by avoiding the UV lamp use.

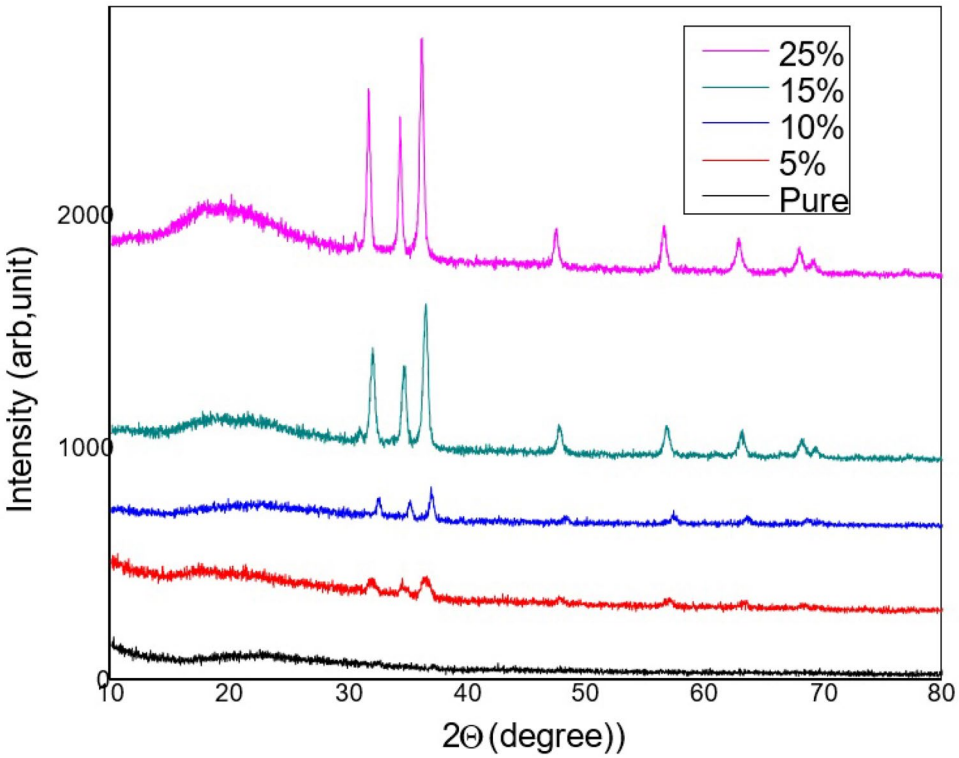

Fig. 3 XRD diffraction pattern recorded in the bioplastic nanocomposite sheets synthetized by casting with incorporation of different IZO nanoparticles weights into the cellulose acetate

An interesting feature that can be deduced from the transmittance spectra is the reduction of the transmittance in the UV (A and B range) i.e. 280–400 nm. The same behavior has been reported also by Culicia et al. [46] in the Ce_2O/CA composite. This suggests the increase of the composite blue radiation absorption with increasing ZnO nanoparticles in CA matrix. This may suggest that the CA filling with ZnO can be a method that improves the UV visible filtering of the CA polymer. The observed increase in the absorption in the UV range may be attributed to the ZnO nanoparticles. Owing a band gap of 3. 17 eV, ZnO absorbs the UV radiations.

Figure 7 shows the FTIR spectra recorded in the frequency range between 400 and 4000 cm^{-1} of different IZO/CA nanocomposite prepared with different weight filler ratio. The whole spectra exhibit peaks located at 1058 cm^{-1} assigned to the C–O vibrational mode, 1234 cm^{-1} assigned to the C–O–C anti symmetric stretching, 1377 cm^{-1} due to C–OH vibration, 1768 cm^{-1} due to C = O carbonyl vibrational stretching vibration and 2380 cm^{-1} due to the C–H group vibration. All these peaks are characteristic of cellulose acetate and assigned respectively to the following bonds vibration. Peaks related to ZnO are not present, only a very small weak peak located at 450 cm^{-1} assigned to ZnO is observed only in the composite prepared with the larger weight filler ratio of 25 wt%. However as shown in Fig. 8, IR peaks are shifted towards the higher wavenumber. This due to change of the bonds environment with including IZO in the CA matrix.

The antibacterial performance of IZO/CA composite against gram-negative *E. coli* and gram-positive *S. aureus* bacterial has been evaluated using the disk diffusion method. Figure 9 show the zone of inhibition (ZOI) obtained in the antimicrobial assays. As can be seen (Fig. 9a), pure CA do not show any antibacterial activity, while IZO/CA composite exhibits significant antibacterial activity against *S. aureus* (Fig. 9a). In Table I is collected the measured ZOI radius in various membranes. The inhibition region varies from 6 to 15 mm with increasing the weight ratio of filler. The same conclusion has been reported by Fahmi et al. [41]. They inferred that the antibacterial activity of the Chitosan/CelAc films increased considerably by adding nano cerium oxide in the films.

The IZO/CA do not exhibit any antibacterial activity against *E. coli*, no halo around the sample was observed (Fig. 9a). The same conclusion has been outlined by Jatoia et al. [37] reported the inactivity of CA/carbon nanotube/Ag against *E. coli* and a significant activity against *S. aureus*. This result agrees with various studies that demonstrated the high sensitivity of gram positive bacterium (*S. aureus*) compared to gram negative bacterium (*E. coli*) vis-à-vis different antibacterial agents [55, 56].

The suggested mechanism of antibacterial activities composite has been based on generation of reactive oxygen

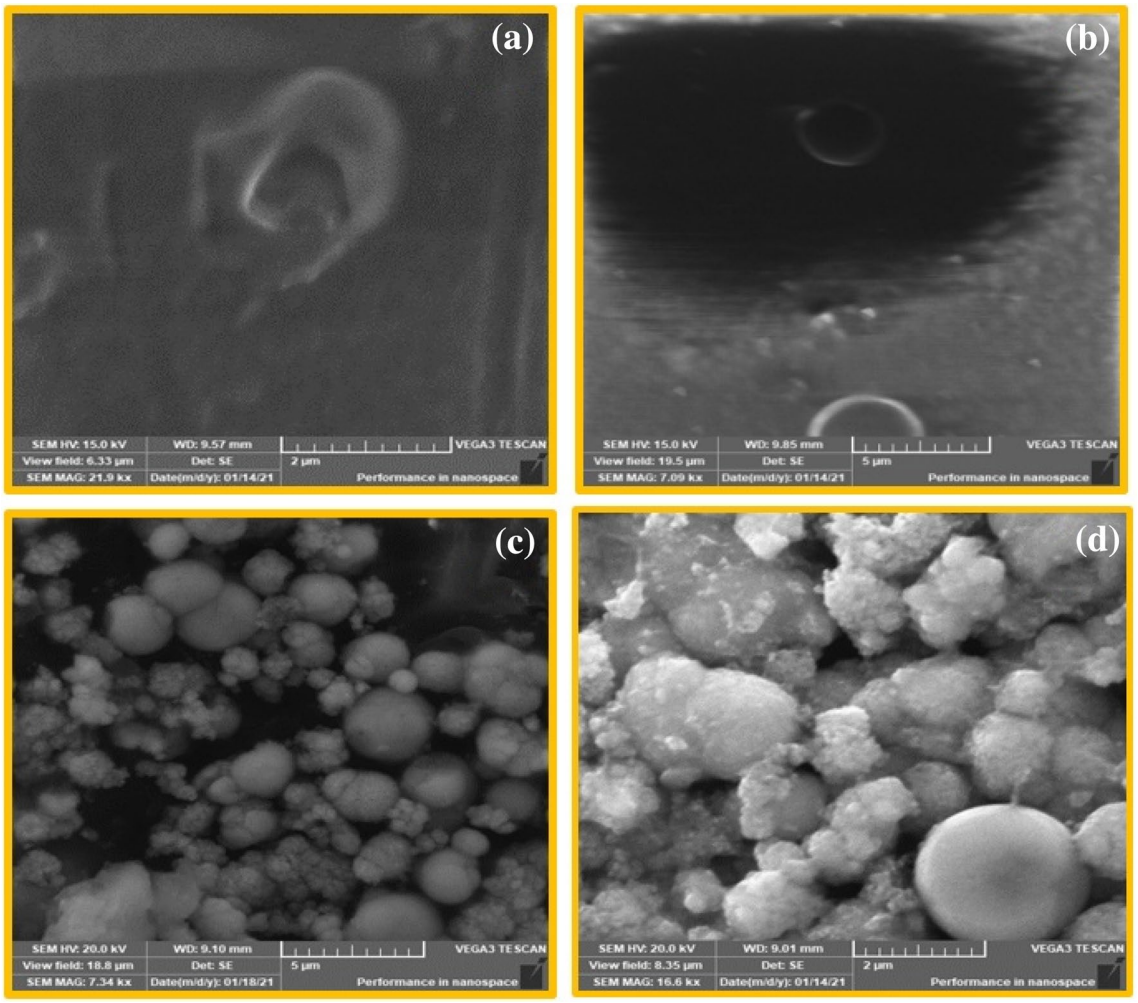

Fig. 4 SEM images of bioplastic nanocomposite sheets prepared with incorporation of different In:ZnO nanoparticles weights into the cellulose acetate **a** pure cellulose acetate polymer, **b** nanocomposite prepared with 5 wt% of IZO nanoparticles, **c** nanocomposite prepared with 15 wt% of IZO nanoparticles and **d** nanocomposite prepared with 25 wt% of IZO nanoparticles

species (ROS), such as hydroxyl, oxide and oxygen radicals which are negatively charged. It was reported that *E. coli* (Gram negative bacteria) cell membranes were more negative and rigid than *S. aureus* [48]. Moreover, *E. coli* enjoys a double lipopolysaccharide membrane that presents a barrier to many substances. Thus owing *E. coli* greater resistance by comparison to *S. aureus* bacteria.

An interesting feature is that the antibacterial performance depends on the film face. Indeed, the synthetized films faces have different color one face is more clear (face A) than the second one (face B) as shown in Fig. 10. The face A do not exhibit any bacterial activity in contrary to the face B (Fig. 10). This may suggest that during the antibacterial assay using the face B, the bacteria is in contact with the antibacterial agent i.e. ZnO nanoparticles, while in the assay with the face A there is no contact with the antibacterial agent. Thereafter, one can conclude that the face B is ZnO rich than the face A. This may be due to the fact that during film casting the nanoparticles, due to the gravity, settle down and condensate at the bottom as shown in the cross section SEM image of the bioplastic sheet (Fig. 11). Thus making the face B ZnO rich and then may explain the different behavior of the films faces regarding the antibacterial activity.

4 Conclusion

In the present we have succeeded in the preparation of bioplastic membrane containing In doped ZnO/cellulose acetate nanocomposite. The influence of weigh ratio of embedded IZO nanoparticles incorporated in the cellulose acetate host matrix. The XRD analysis and the SEM observations reveal that the IZO nanoparticles are well introduced in the acetate

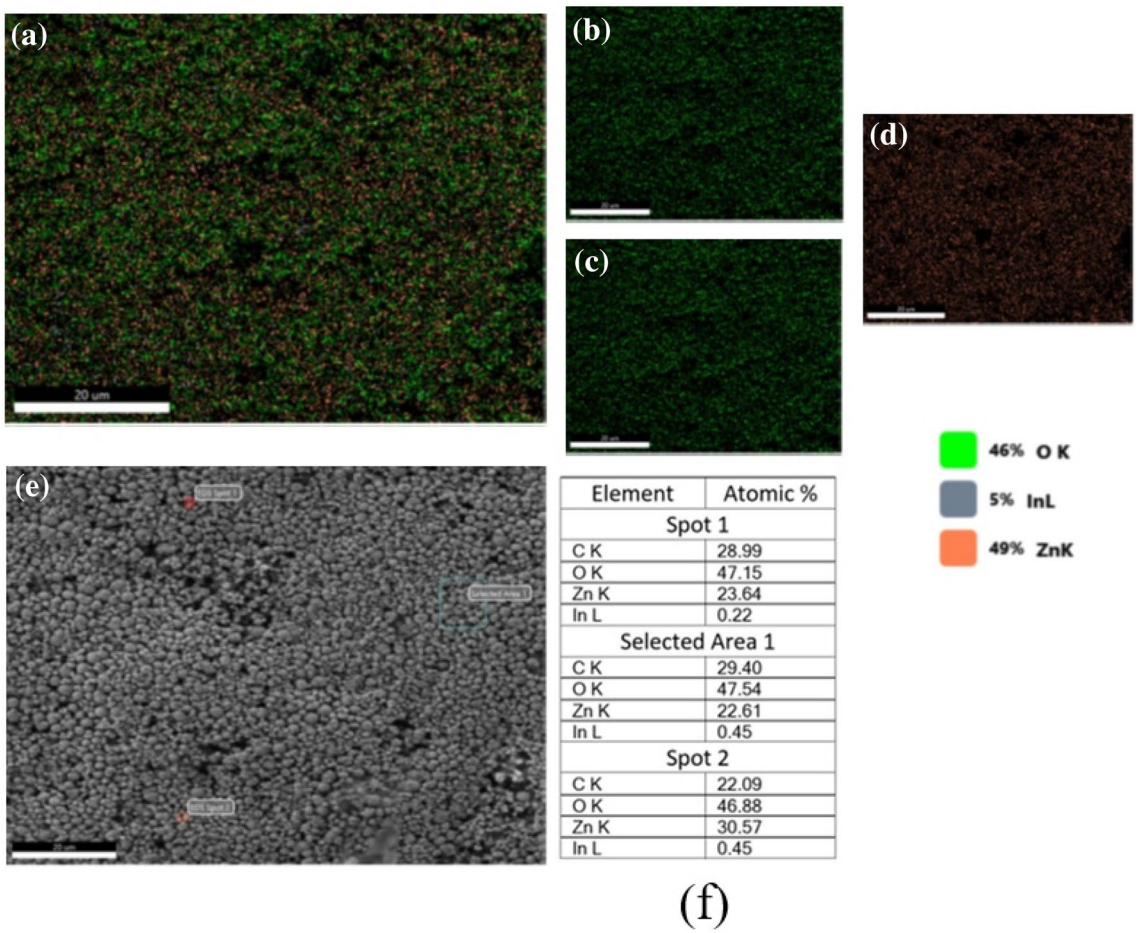

Element	Atomic %
Spot 1	
C K	28.99
O K	47.15
Zn K	23.64
In L	0.22
Selected Area 1	
C K	29.40
O K	47.54
Zn K	22.61
In L	0.45
Spot 2	
C K	22.09
O K	46.88
Zn K	30.57
In L	0.45

Fig. 5 Elements composition mapping **a** EDX mapping of whole elements, **b** EDX mapping of Zn element, **c** EDX mapping of oxygen and **d** indium, **e** and **f** EDX composition in three different spot regions

network and well uniformly dispersed in the whole polymer matrix according to the EDX element mapping observation. The synthetized membrane was tested against the gam positive (*S. aureus*) and gam negative (*E. coli*) bacteria. The optical characterization reveals the reduction of the transmittance in the UV (A and B range) of the CA/IZO composite with increasing the weight of the added IZO powder. This reduction was attributed to ZnO UV absorption. No noticeable peak assigned to ZnO bond are observed. However, IR peaks are shifted towards the higher wavenumber due to the change of the bonds environment with including IZO in the CA matrix. From the assay tests we concluded that the IZO/CA nanocomposite has a good antibacterial activity against gam *S. aureus*, the inhibition region varies from 6 to 15 mm with increasing the weight ratio of IZO filler weight. While, no antibacterial activity against *E. coli* bacteria was detected. Moreover, due the nanoparticles settlement at the bottom of the preparation Petri dish during polymer casting, the synthetized polymer has an active face (containing ZnO nanoparticles) and inactive face (free from ZnO nanoparticles).

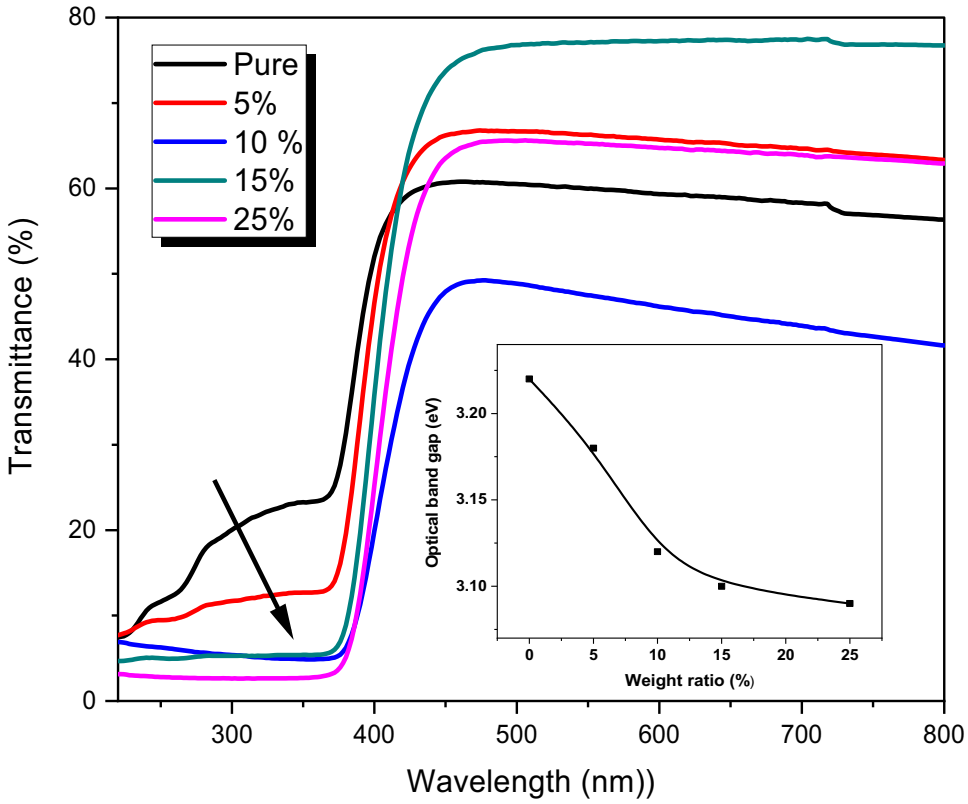

Fig. 6 UV–Vis transition spectra recorded in the different synthetized bioplastic nanocomposites. Insert figure shows the correlation between the nanocomposite band gap and the added weight of the nanoparticles

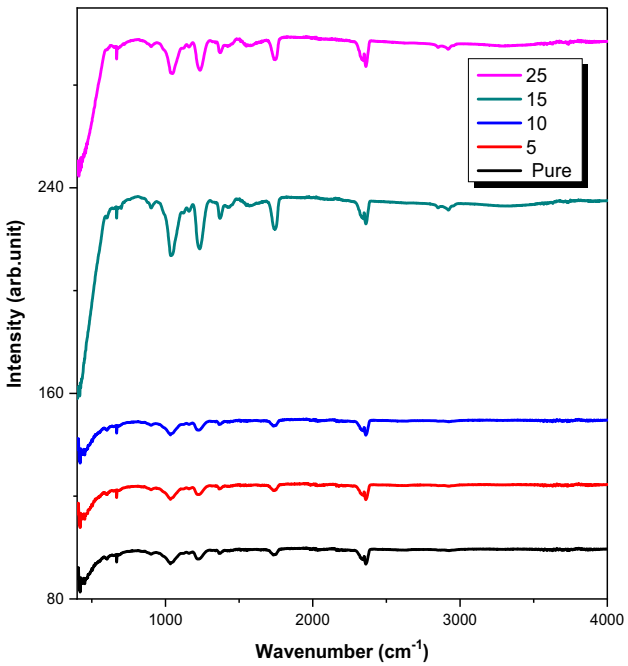

Fig. 7 FTIR spectra recorded in the different synthetized bioplastic nanocomposites

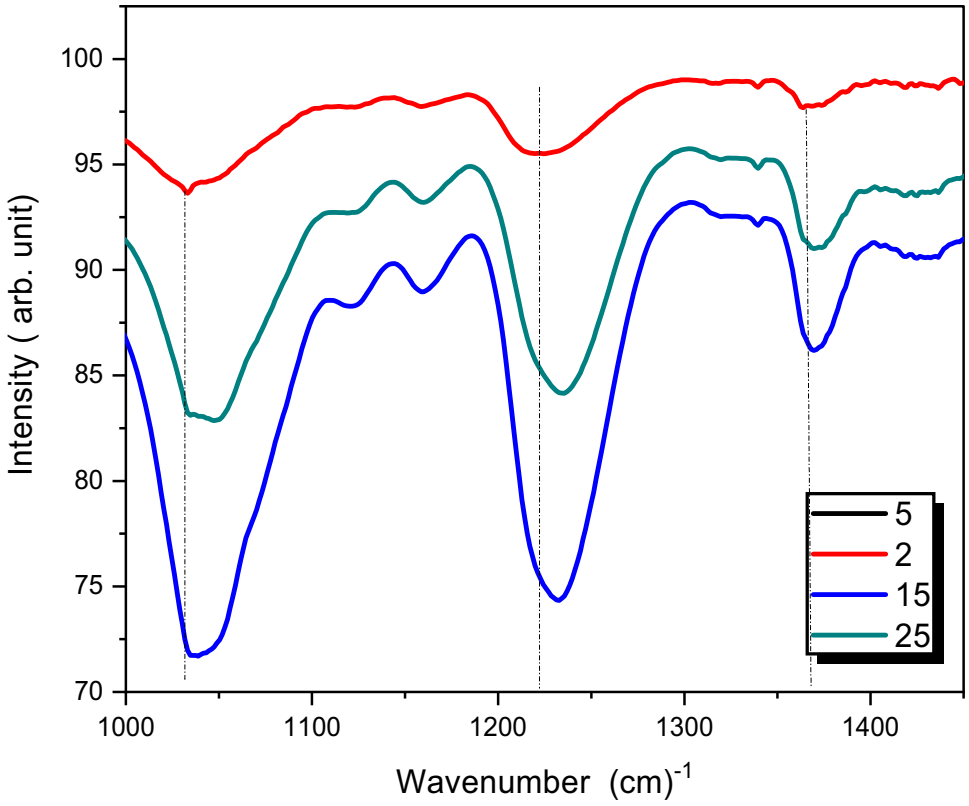

Fig. 8 Reduced range FTIR spectra recorded in the different synthetized bioplastic nanocomposites showing the different IR peak shifts

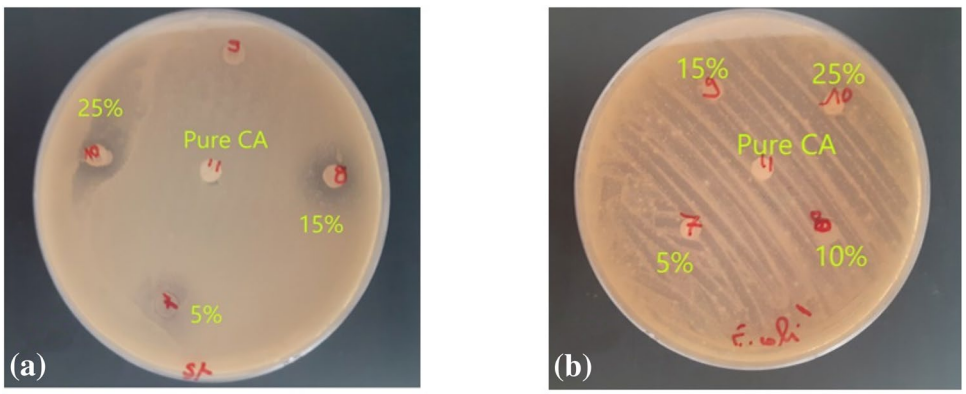

Bacteria	Weight ratio (%)	ZOI
S. Aureus	5%	6mm
	10%	10mm
	15%	14mm
	25%	16mm

(c)

Fig. 9 Agar plates containing zones of inhibition obtained with different disc cut from various bioplastic samples of tested bacteria's **a** *S. aureus* and **b** *E. coli*, **c** the measured ZOI diameter achieved by different samples prepared with various IZO nanoparticles weight ratios against *S. aureus* bacteria

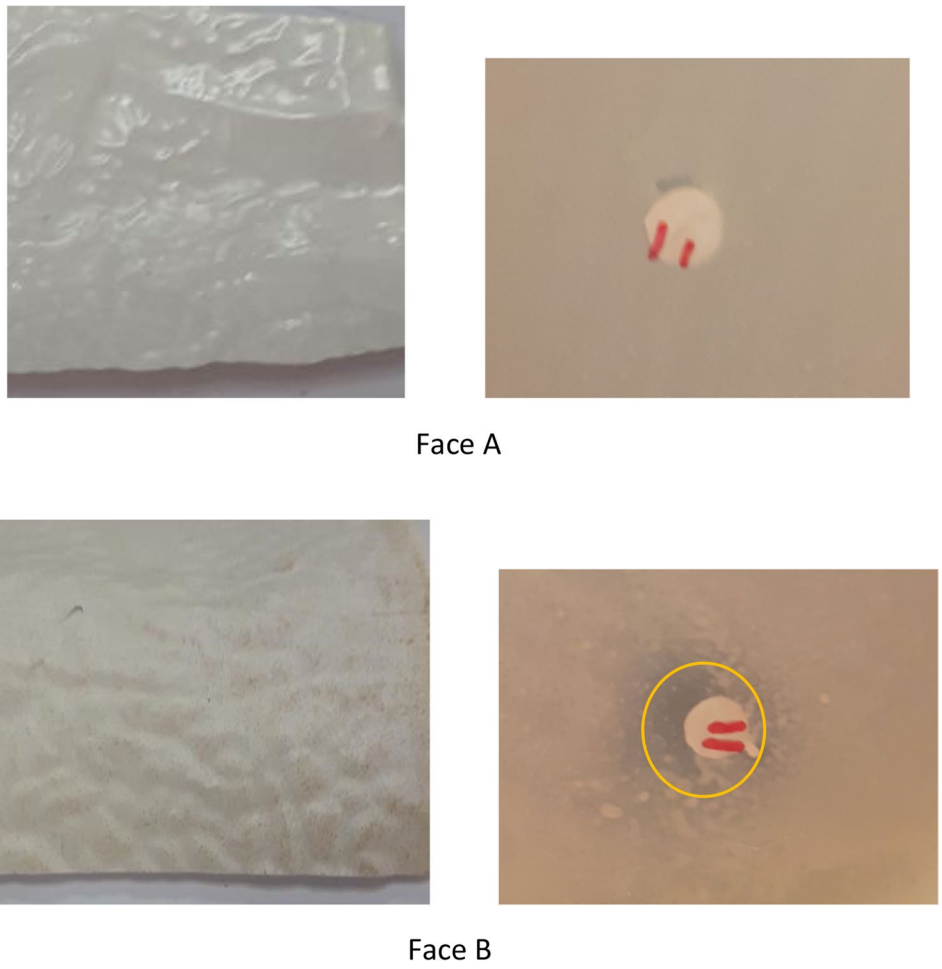

Fig. 10 Photo and ZOI image of different faces of a nanoplastic sheet: **a**, **b** face A and **c**, **d** face B

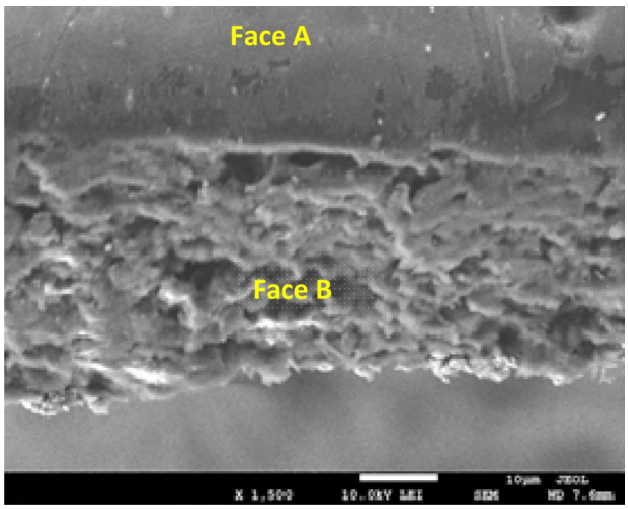

Fig. 11 Cross sectional SEM image of a bioplastic sheet showing the settlement of IZO nanoparticles in one side of the sheet

Acknowledgements This research work was funded by institutional Fund Projects under Grant number (IFPRC-197-130-2020). Therefore, authors gratefully acknowledge technical and financial support from the Ministry of Education and King Abdulaziz University, Jeddah Saudi Arabia.

Declarations

Conflict of interest The authors declare that they have no conflict of interest.

References

1. L.E. Aguilar, A. Ghavami Nejad, C.H. Park, C.S. Kim, Nanomedicine **13**(2), 527 (2017)
2. G. El-Barbary, M.K. Ahmed, M.M. El-Desoky, A.M. Al-Enizi, A.A. Alothman, A.M. Alotaibi, A. Nafady, Synth. Met. **278**, 116824 (2021)

3. S. Beis, S. Monteiro, R. Santos, A.S. Figueiredo, M. Guadalupe, M. Sanchez-Loredo, M.A. Lemos, F. Lemos, M. Minhalma, M. Norberta de Pinho, Water Res. **149**, 225 (2019)
4. Y. Wu, G. Xu, W. Zhang, C. Song, L. Wang, X. Fang, L. Xu, S. Han, J. Cui, L. Gan, Carbohydr. Polym. **267**, 118166 (2021)
5. J. Lostea, J.-M. Lopez-Cuesta, L. Billona, H. Garay, M. Save, Progress Polym. Sci. **89**, 133 (2019)
6. M. Abbas, M. Buntinx, W. Deferme, R. Peeters, Nanomaterials **9**, 1494 (2019)
7. M. Choi, G. Murillo, S. Hwang, J.W. Kim, J.H. Jung, C.Y. Chen, M. Lee, Nano Energy **33**, 462 (2017)
8. E. Tang, S. Dong, Colloids Polym. Sci. **287**, 1025 (2009)
9. S. Tachikawa, A. Noguchi, T. Tsuge, M. Hara, O. Odawara, H. Wada, Materials **4**, 1132 (2011)
10. S. Li, M.M. Lin, M.S. Toprak, D.K. Kim, M. Muhammed, Nano Rev. **1**, 1 (2010)
11. S. Zinatloo-Ajabshir, S.A. Heidari-Asil, M. Salavati-Niasari, Sep. Purif. Technol. **280**(1), 119841 (2022)
12. H. Etemadi, S. Afsharkia, S. Zinatloo-Ajabshir, E. Shokri, Polym. Eng. Sci. **61**, 2364–2375 (2021)
13. S. Zinatloo-Ajabshir, M. Mousavi-Kamazani, Ceram. Int. **47**(17), 23702–23724 (2021)
14. H. Safajou, M. Ghanbari, O. Amiri, H. Khojasteh, F. Namvar, S. Zinatloo-Ajabshir, M. Salavati-Niasari, Int. J. Hydrogen Energy **46**(39), 20534–20546 (2021)
15. S. Sharaf, M.E. El-Naggar, Cellulose **25**(9), 5195–5204 (2018)
16. M.S. Abdelrahman, T.A. Khattab, A. Aldalbahi, M.R. Hatshan, M.E. El-Naggar, J. Environ. Chem. Eng. (2020). https://doi.org/10.1016/j.jece.2020.104573
17. A. Aldalbahi, M.E. El-Naggar, M.K. Ahmed, G. Periyasami, M. Rahaman, A.A. Menazea, J. Mater. Res. Technol. **9**, 15045 (2020)
18. A. Aldalbahi, M. El-Naggar, T. Khattab, M. Abdelrahman, M. Rahaman, A. Alrehaili, M. El-Newehy, Polymers **12**, 2501 (2020)
19. A. Abdel-Karim, M.E. El-Naggar, E.K. Radwan, I.M. Mohamed, M. Azaam, E.R. Kenawy, Chem. Eng. J. **405**, 126964 (2021)
20. A. Zucchelli, M.L. Focarete, C. Gualandi, S. Ramakrishna, Polym. Adv. Technol. **22**, 339–349 (2011)
21. A.R. Unnithan, G. Gnanasekaran, Y. Sathishkumar, Y.S. Lee, C.S. Kim, Carbohydr. Polym. **102**, 884 (2014)
22. T.J. Sill, H.A. von Recum, Biomaterials **29**, 1989 (2008)
23. S. Tungprapa, I. Jangchud, P. Supaphol, Polymer **48**, 5030 (2007)
24. T.P. Armedya, M.F. Dzikri, S.C.W. Sakti, A. Abdulloh, Y. Raharjo, S. Wafiroh, M.Z. Fahmi, BioNanoScience **9**, 274 (2019)
25. A.W. Jatoi, Z. Khatri, F. Ahmed, M.H. Memon, J. Surf. Deterg. **18**, 205 (2015)
26. A. W., Jatoi, I. S. Kim, and Q.Q. Ni, Appl. Nanoscience, 1 (2018)10.
27. H. Lee, A.W. Jatoi, Y. Kyohei, K.-O. Kim, K.H. Song, J. Lee, Text. Res. J. **88**, 630 (2018)
28. A.R. Unnithan, G. Gnanasekaran, Y. Sathishkumar, Y.S. Lee, C.S. Kim, Carbohyd. Polym. **102**, 884 (2014)
29. S.K. Nethi, S. Das, C.R. Patra, S. Mukherjee, Biomater. Sci. **7**, 2652 (2019)
30. S. Subhadarshini, R. Singh, D.K. Goswami, A.K. Das, N.C. Das, Langmuir **35**(52), 17166–17176 (2019)
31. S. Subhadarshini, R. Singh, A. Mandal, S. Roy, S. Mandal, S. Mallik, D.K. Goswami, A.K. Das, N.C. Das, Langmuir **37**(31), 9356–9370 (2021)
32. S. Subhadarshini, E. Pavitra, G.S.R. Raju, N.R. Chodankar, D.K. Goswami, Y.-K. Han, Y.S. Huh, NCh. Das, A.C.S. Appl, Mater. Interfaces **12**(26), 29302–29315 (2020)
33. S. Subhadarshini, E. Pavitra, G.S.R. Ma Raju, N.R. Chodankar, A. Mandal, S. Roy, S. Mandal, M.V. Basaveswara Rao, D.K. Goswami, Y. Suk Huh, N.C. Das, Ceram. Int. **47**(11), 15293–15306 (2021)
34. S. Beisl, S. Monteiro, R. Santos, A.S. Figueiredo, M.G. Sanchez-Loredo, M.A. Lemos, F. Lemos, M. Minhalma, M. Norberta de Pinho, Synth. Met. **278**, 116824 (2021)
35. M.R. Amin, M.A. Chowdhury, M.A. Kowser, Heliyon **5**, 02009 (2019)
36. S.I. Al-Saeedi, N.S. Al-Kadhi, G.M. Al-Senani, O.A. Almaghrabi, A. Nafady, Int. J. Biol. Macromol. **182**, 464 (2021)
37. A.W. Jatoi, H. Ogasawara, I.S. Kim, Q.Q. Ni, Mater. Sci. Eng. C **110**, 110679 (2020)
38. J.R. Ricardo, I.P. Matos, C. Chaparro, J.C. Silva, M.A. Valente, J.P. Borges, P.I. Soares, Carbohydr. Polym. **198**, 9 (2018)
39. M.K. Ahmed, A.A. Menazea, A.M. Abdelghany, Int. J. Biol. Macromol. **155**, 636 (2020)
40. A.A. Aly, M.K. Ahmed, Int. J. Pharm. **598**, 120325 (2021)
41. M.Z. Fahmi, R.A. Prasetya, M.F. Dzikri, S. Candra, W. Sakti, B. Yuliarto, I. Ferdiansjah, Mater. Chem. Phys. **250**, 123055 (2020)
42. Z. Kalaycıoğlu, N. Kahya, V. Adımcılar, H. Kaygusuz, E. Torlak, G. Akın-Evingür, F.B. Erim, Eur. Polym. J. **133**, 109777 (2020)
43. A.A. Badawy, A.F. Ghanem, M.A. Yassin, A.M. Youssef, M.H. Abdel Rehim, Environ. Nanotechnol. Monit. Manage. **16**, 0501 (2021)
44. M.K. Haider, A. Ullah, M. Nauman Sarwar, Y. Saito, L. Suna, S. Park, I.S. Kim, Int J. Biol. Macromol. **173**, 315–326 (2021)
45. Z. Lu, J. Gao, Q. He, J. Wu, D. Liang, H. Yang, Carbohydr. Polym. **156**, 460 (2017)
46. P.K. Dutta, S. Tripathi, G.K. Mehrotra, J. Dutta, Food Chem. **114**, 1173 (2009)
47. I.S. Elashmawi, E.M. Abdelrazek, A.M. Hezma, A. Rajeh, Phys. B Condens. Matter **434**, 57 (2014)
48. E.M. Abdelrazek, I.S. Elashmawi, A. Hezma, A. Rajeh, Int. J. Modern Appl. Phys. **1**, 83 (2012)
49. S.M. Hassan, A.I. Ahmed, M.A. Mannaa, Ceram. Int. **44**, 6201 (2018)
50. R. Brayner, R. Ferrari-Iliou, N. Brivois, S. Djediat, M.F. Benedetti, F. Fievet, Nano Lett. **6**, 866 (2006)
51. G.X. Tong, F.F. Du, Y. Liang, Q. Hu, R.N. Wu, J.G. Guan, X. Hu, J. Mater. Chem. B **1**, 454 (2013)
52. R.R. Krishna, T.K. Ranjit, C.M. Adhar, Langmuir **27**, 4020 (2011)
53. J. Nicole, R. Binata, T.R. Koodali, C.M. Adhar, Microbiol. Lett. **279**, 71 (2008)
54. M.E. Culica, A.L. Chibac-Scutaru, V. Melinte, S. Coseri, Materials **13**, 2955 (2020). https://doi.org/10.3390/ma13132955
55. K. Ravichandrana, R. Rathia, M. Banetoc, K. Karthikaa, P.V. Rajkumara, B. Sakthivela, R. Damodaran, Ceram. Int. **41**, 3390 (2015)
56. S. Anithaa, S. Muthukumaran, Mater. Sci. Eng. C **108**, 110387 (2020)